Journal of Engineering and Computer Sciences, Qassim University, Vol. 2, No. 2, PP 135-146 (July 2009/Rajab 1430H.)

Theoretical Characteristics of Quantum Cascaded Lasers

A. Nasr[1], M. B. El-Mashade[2] and M. El-Tokhy[3]
[1]*Radiation Engineering Dept., NCRRT, Atomic Energy Authority (AEA), Egypt*
[1]*Computer Eng. Dept., Computer College, Qassim Uinv. Saudi*
[2]*Elect. Eng. Dept., Faculty of Eng., Al_Azhar Univ., Egypt.*
[3]*Engineering dept., NRC, AEA, Egypt*
[1]*ashraf.nasr@gmail.com* [3]*engtokhy@gmail.com*

(Received 26/12/2008; accepted for publication 12/3/2009)

Abstract. In this paper, we are concerned with the performance of the quantum cascaded lasers (QCLs) under two different cases, pulsed and continuous wave (PW, CW) operations. The dependence of PW and CW on QCLs parameters is declared. These parameters are width of the strip, number of stages and wavelengths. Also, proposed relations that link emitted power, threshold current, and slope efficiency with QCLs parameters are deduced. To verify the validity of these theoretical equations, comparison studies with experimental results are done. From comparison of the theoretical and experimental characteristic behaviors, the considered equations give satisfactory results. Furthermore, mathematical approximation for the maximum and minimum values of the output optical power is deduced.

Key Words: Threshold current / number of stages / population inversions / laser power / Injection and active regions.

1. Introduction

QCLs are new light sources based on intersubband transitions in QWs that have led to laser action over most of the mid-infrared (MIR) and part of the far-infrared (FIR) spectrum [1-5]. The advent of the quantum cascade lasers (QCLs) with emission wavelengths available in the infrared range from 3 μm through more than 100 μm opens up the possibility of exploiting infrared atmospheric transparency windows for free space optical communications [6], trace gas analysis for pollution monitoring, environmental sensing, medical diagnostics (e.g. breath analyzers), automobile applications such emission control, cruise control and collision avoidance radar, military applications; such as countermeasures, and wireless optical communications .

Additionally, the trend in the world was directed towards the quantum cascaded lasers because they have a several advantages over conventional laser diode, such as their high speed digital modulation and results on MIR optical wireless communication links, which demonstrate the possibility of reliably transmitting complex multimedia data streams [7]. There are many relevant points that make this kind of device so unique. The most important point is the multistage cascade scheme, where electrons are recycled from one period to another, contributing each time to the gain and the photon emission. Thus each electron injected above threshold can emit as many photons as the number of QW constituting the cascading scheme, leading to a differential efficiency and therefore an optical power proportional to the period, N_p. The other point is the unipolarity of QCLs. The initial and final states of the electrons are only in the conduction band and therefore have the same curvature in the reciprocal space. And as a third important feature, the intersubband gain is only limited by the quantity of carriers that can be injected in the upper state and does not saturate as it happens for interband lasers. The next fundamental trait is that the emission wavelength is not dependent on the band gap of constituent materials, but can be tuned simply by tailoring the layer thickness. At present, QCLs are the only semiconductor lasers that operate at room temperature and above in pulsed mode at several MIR wavelengths. As well as, they do not involve the band-gap of the material for the generation of light. Therefore, InP- and InGaAs -based III–V semiconductor materials can now be used for the generation of long-wavelength for mid-infrared light. Furthermore, these materials are straightforward to process and pattern. This is essential for the more sophisticated device geometries such as distributed feedback lasers (DFB) [8]. There are many kinds of optical transition that are employed in the active regions of QCLs. Firstly; the vertical transition maximizes the wavefunction overlap, resulting in a strong dipole coupling between the two states. Generally, vertical transitions are delocalized over single well and present the narrowest spontaneous emission linewidths *(~1meV).* The drawback is that the strong wavefunction overlap decreases the upper state lifetime, calling for an efficient depletion mechanism for the lower state. One variant of the vertical transition that proves to be highly efficient is the two-well vertical transition, here, the optical transition is still vertical but the wavefunction is delocalized over two wells. Further, the luminescence linewidth is kept quite broad *(~ 4 meV)* with the advantage of a better design for the extraction of the carriers from the lower state, i.e. the lifetimes of the electrons in state number two, τ_2 will be decreased [9]. The optical transition can also be made more "diagonal" in real space; reducing the overlap with the lower state. Either by anticrossing the excited state of one quantum well with the ground state of a neighboring one, or by relying on a photon assisted tunneling transition. The upper state lifetime of the electrons between state 3 and two; τ_{32}, will then increase, and also decreases the escape rate $(t_{esc})^{-1}$ of electrons into the continuum at the expenses of a weaker dipole and a broader luminescence linewidth. As a third point optical transitions between edge states of a miniband, like in the chirped superlattice design, present high values of the oscillator strength but the injection selectivity is reduced. Also, in this case, due to the large delocalization of the wavefunction, typical values of electroluminescence linewidth are higher than in the vertical case *(~2 meV)*. The latter, the bound-to-continuum optical transition is slightly more diagonal than the superlattice one. Due to the choice of having one isolated upper state. In this case, there is some more control in the upper state lifetime by tuning the first barrier thickness. And typical value of the luminescence linewidth is in the *2 meV* range. The price to pay is lower oscillator strength with respect to the superlattice case.

In this manuscript, the power and threshold current density for pulsed and continuous mode operation are discussed in details. The main target of our work is to improve the characteristic of QCLs, by reducing the threshold current density as much as possible and increasing the emitted power. Also, we will describe the temperature dependence of the threshold current density. Moreover, the increase of power with the current which represent the slope efficiency will be explained. In section *2,* we present the basic assumptions and model description. Performance analyses of QCLs including threshold current density, radiated power, and slope efficiency are considered in section *3*. We summarize our numerical results in section *4* and we terminate our study with a brief discussion, stating some important conclusions that we note from our obtained results.

2. BASIC ASSUMPTIONS AND MODEL DESCRIPTION

QCLs under consideration are complex devices, whose core is a multiple quantum wells (MQWs) [1-5, 10], containing a series of repeated InGaAs wells sandwiched between much thicker layers of the alloy semiconductor InAlAs barriers. We assume that each quantum well (QW) contains three subband levels. The transitions between these subbands is called an intersubband transitions [11]. These intersubband levels are at equilibrium in the case of no bias and reach the flat condition (as a staircase), when the correct bias is applied. In our model, the thermal effect of mobile carriers and thermally populated injector states of energy width is neglected. To compare the theoretical results with its analogous experimental results, the QCLs parameters are chosen similar to the case of experimental state. As depicted in figure (1-a), the device; realized by InGaAs/InAlAs lattice matched to InP, is constituted by one basic structure, called period, N_p, which can be repeated several times. This process allows electron recycling that can be re-injected in the subsequent period. One period is then split in an active region, where the optical transition occurs and relaxation-injection region, whereas the carriers can relax after having completed the optical transition. Besides, the injector region is doped, acting as an electron reservoir and so it re-inject the electrons in the next period. As seen in figure (1-b), the injector and the active region are under the correct bias. The carriers are injected from this injector region by resonant tunneling in the upper lasing state of the active region, state $|3\rangle$, where they can relax to state $|2\rangle$ by means of photon-assisted tunneling or by scattering, mainly from longitudinal (LO) phonon if the condition $E_{32} \geq \hbar w_{lo}$ is satisfied, where, E_{32} is the energy gap between state 3 and 2, $\hbar w$ is emitted energy from longitudinal. The most striking point is the achievement of the population inversion by careful quantum engineering of the lifetimes of the states (typically in the pico second (ps) range), while in an interband laser the inversion condition comes from an intrinsic property of the material. In order to achieve population inversion, the lifetimes of the electrons in the QCL states must satisfy the relation $\tau_{32} \succ \tau_2$. This condition is achieved by means of two key points:

1. The lifetime τ_{32} is increased by employing a transition with a reduced spatial overlap of the wavefunctions.

2. The lifetime τ_2 is reduced by making the energy E_{21} resonant with the optical phonon energy that is the most efficient scattering mechanism.

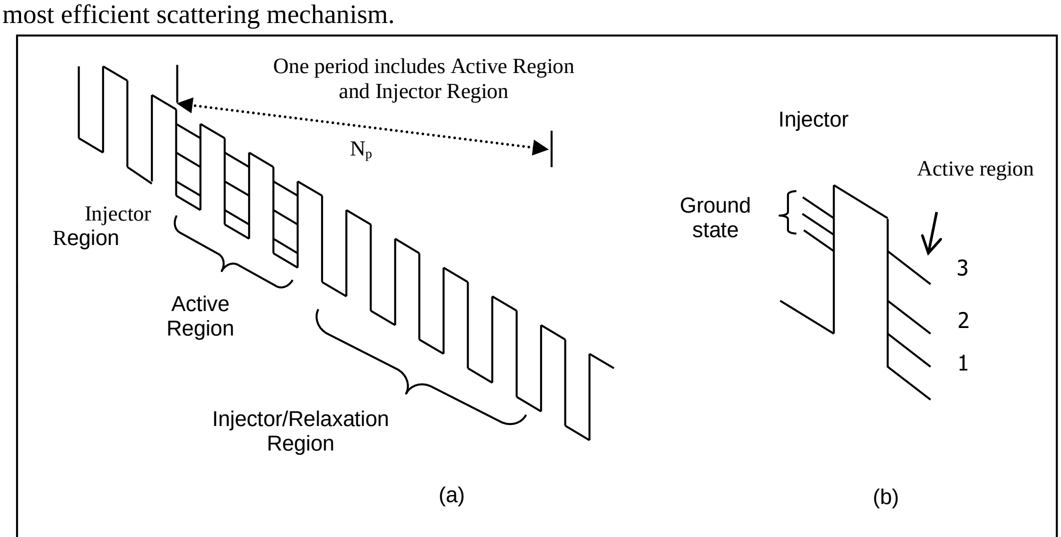

Fig. (1). (a). Quantum cascaded lasers design InGaAs(wells) / InAlAs (barriers).
(b). Active and injector region under bias.

In our model we have employed the vertical optical transitions using three quantum wells. These transitions occur inside the active region. The Injector region contains five QWs that will be assumed equal in their widths and lengths. The excitation energy between states 2 and 1 in each one is assumed to be comparable with the phonon energy (~36meV). The applied biasing voltage should be sufficient to cause a tunneling into QCLs. In most cases of QCLs, the internal efficiency is assumed to be equal one. The characteristic temperature, T_o, for InGaAs ranges from 40 -75 K. In our point under research, T_o=55K is chosen for comparison with the experimental studies. A schematic diagram of QCL device is depicted in figure (2). It is mounted on a copper carrier. The carrier has one or two ceramic pads carrying the bonding wires. The pads are yellow on top due to a layer of gold, and white around it and on the sides which is the color of the ceramic. If these pads are placed upwards, the vertical for the laser is the same as the observer vertical direction. If there are two ceramic pads present, they are named, as in figure 2, up pad and down pad. Looking onto the front facet with the laser placed as described above, the pad left of the laser chip is called "down", and the one right of it "up". The cathode is connected to the ceramic pads and the anode is connected to the copper Carrier. We assume that pulsed QCLs need pulse current up to *10A*, voltage up to *12V* and, maximum rise/fall time of *10ns* to prevent detrimental heating. A CW QCL is about as sensitive to electrical surges and instabilities as a conventional bipolar laser diode. It is necessary to use a good quality power supply to ensure, current and voltage are stable within 0.1%. Generally the operating voltage for CW is in the *8V- 12V* range and current in the *0.5A-1.5A* range [12].

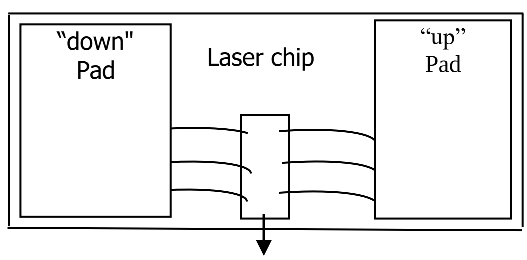

Fig. (2). QCL device with emission from front facet.

3. Performance Analysis of Quantum Cascaded Laser

1. OUTPUT POWER

A useful measure describing the performance of QCLs is the output power. It is a measure that takes into account the internal efficiency as well as QCLs different parameters. The proposed mathematical expression that describes the relation between output optical power and QCLs parameters is as the following:

$$p = A\left(j - j_{th}\right)e^{T/T_o}\frac{\hbar\nu}{e}N_P\frac{\alpha_m}{\alpha_m + \alpha_w}\eta_i \tag{1}$$

The relation specifies the dependence of optical power on the threshold current density. While; A denotes the strip area (cm^2), j denotes the injected current density (KA/cm^2), h denotes the Plank's constant, ν denotes the frequency, e denotes the electron charge, α_m denotes the mirror losses (cm^{-1}), α_w denotes the waveguide losses (cm^{-1}), η_i denotes the internal efficiency.

2. THRESHOLD CURRENT DENSITY

Laser threshold is the smallest amount of injected current necessary for obtaining lasing effect. Or it is a minimum amount of gain necessary for the operation of laser. This amount can be realized only when the laser is pumped above a threshold level. The current needed to reach the threshold is called the threshold current density J_{th} [13]. In all cases it is more practical to have a very small amount of the threshold current density. The temperature dependence of the threshold current for QCLs can be expressed by an exponential fit as stated in [14]:

$$j_{th} = j_{th}(0)e^{T/T_o} \tag{2}$$

From the mathematical model the threshold current density is given by the following relation:

$$j_{th} = j - \frac{pe(\alpha_m + \alpha_w)}{A\hbar\nu N_P \alpha_m \eta_i} e^{-T/T_o} \tag{3}$$

Where; J_{th} denotes the threshold current density at a certain temperature (KA/cm^2), $J_{th}(0)$ denotes the threshold current density at zero, T_0 denotes the characteristic temperature of the compound materials, T denotes the absolute temperature (K).

3. SLOPE EFFICIENCY

The slope efficiency, which can be defined as $\partial p / \partial i$, i.e. can be defined as the increase in output laser power per unit current increase above threshold. It can be also represented as the number of photons generated per electron above laser threshold and it is given by the following relation [15]:

$$\frac{\partial p}{\partial i} = \frac{\hbar\nu}{2e} \frac{N_P \alpha_m}{\alpha_w + \alpha_m} \eta_i \tag{4}$$

Hence, $h\nu$ is the photon energy in (meV)

From equation (5), the total external differential quantum efficiency; which is collected from both facets, can be calculated as

$$\eta_d = \left(\frac{2e}{\hbar\nu}\right)\left(\frac{\partial p}{\partial i}\right) = \frac{N_P \alpha_m}{\alpha_w + \alpha_m} \eta_i \tag{5}$$

4. Results and Discussions

In this section, we give some numerical results of pulsed and continuous mode operations for the considered QCLs. At first, we compare between theoretical and practical results for pulsed waves (PW) mode operation. The output power versus threshold current for the laser operated in PW at 80 and 300K are shown in figure (3) for a wide stripe. From the figure, one can observe that as the temperature increases the threshold required for obtaining lasing effect is increased.

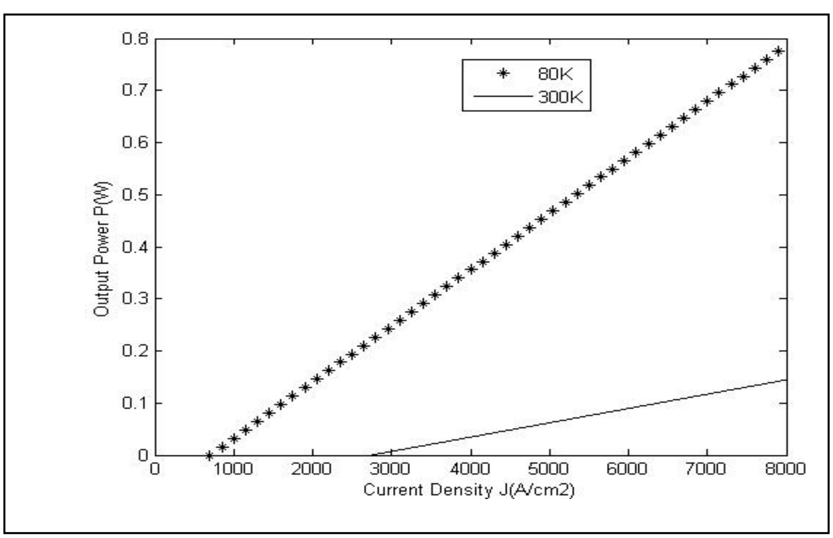

Fig. (3). Radiated optical Power vs. J, at different temperature for PW.

In the same time, the emitted power is reduced substantially with the operating temperature. Also, for one value of temperature, the emitted power is directly proportional to the current density. The obtained theoretical results support experimental one; as in [16]. Table (1) gives this numerical comparison between output optical power at different values of operating temperatures and current densities.

The remind factor at (PW) operation is the slope efficiency and differential efficiency. Its value ($\partial p / \partial i$) equals 31.4 (*mW/A*). We can observe that the value of slope efficiency is a measure of the performance enhancement of the QCLs under investigation. While, differential efficiency equals 0.36.

Table (1). denotes a comparison between theoretical and experimental output power, P, for pulsed operation.

		Theoretical	**Practical**
T	**J (A/cm^2)**	P (W)	P (W)
80K	5125	0.5428	.342
300K	7500	.171	.16
300K	5125	.09	.09

In the second case, for (CW) operation, we employed two wide strips 14 μ m and 20 μ m. At 14 μ m wide stripe, the dependence of the emitted power behavior on the threshold current at different operating temperatures is shown in figure (4). We notice that the emitted power decreases with increasing the temperature which verifies the experimental results as in [16]. The calculated slope efficiency for (CW) operation at 14 μ m per facet is .067 *W/A*, and corresponding differential quantum efficiency per period is 0.783. Similarly as in part one, Table (2) gives a comparison between our theoretical and experimental results as in [16] for the same parameters defined in Table 1; T(K) and J(KA/cm^2).

Table (2). denotes a comparison between theoretical and experimental output power, P, for strip width 14 µm in the case CW operations.

		Theoretical	**Practical**
T(K)	**J (kA/cm^2)**	P (W)	P(W)
140	2.01	0.0328	.025
160	2.16	0.019	.0125
180	3.082	0.016	.01

Finally for 20 μm wide strip, the output power versus the threshold current density for CW operation is shown in the figure (5). Similarly as in the case of 14 μm , the emitted power for smaller operating temperatures is larger than that for higher temperatures, as well, j_{th} is increased with temperatures.

Table (3). denotes a comparison between theoretical and experimental output power, P, for strip Width 20 µm in the case CW operations.

		Theoretical	**Practical**
T(K)	J (kA/cm^2)	P (W)	P(W)
120	1	0.0056	0.005
140	1.5	0.01	0.01250

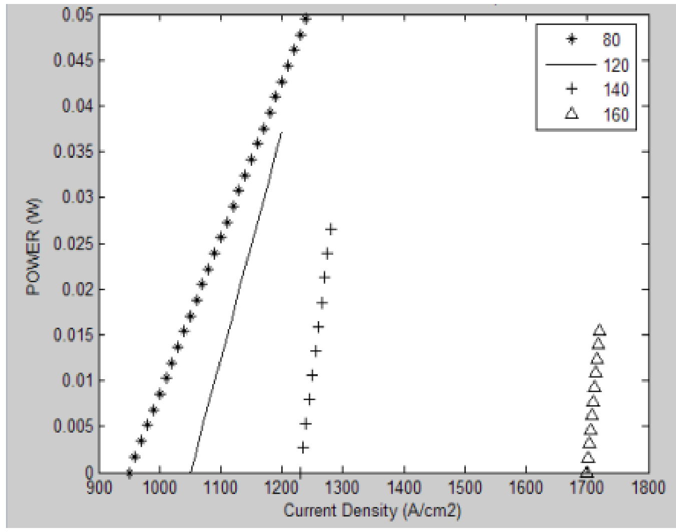

Fig. (4). Radiated Power vs J_{th} at different temperatures for 14 μm, theoretically.

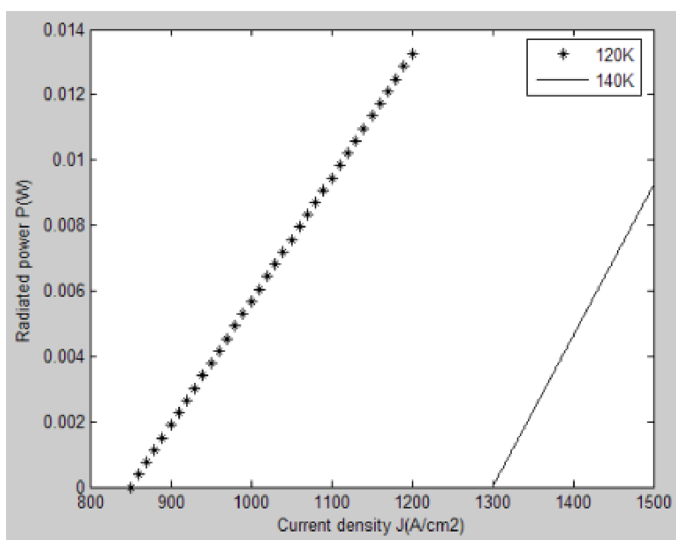

Fig. (5). Radiated Power vs J_{th} at different temperatures for 20 μm, theoretically.

Additionally the measured slope efficiency for CW operation at 20 μ m per facet is 0.142 W/A [16], and as a result of this, the differential quantum efficiency per period is η_d = 1.644. In general, the resulting external differential quantum efficiency is greater than unity only in lasers with cascaded active regions as in [17].

Now we will examine the temperature dependence of the laser threshold current density in the range from *0* to *140 K* for T_0*=53 K and* T_0*=100 K*. As shown in figure (6), we notice that when the operating temperature increases, for both two characteristic temperatures, the threshold current increases and consequently the optical power is reduced, as depicted in figure 11, which support this idea. As well as, evident from figure (6), J_{th} is lower for higher characteristic temperature (T_0) than that for smallerT_0. This process allows high-power operation particularly at higher temperatures.

From the investigation of the proposed equation (2), and the obtained figures (7 and 8), the emitted optical power of QCLs can be increased by adjusting two parameters, number of periods; N_p, and *strip area;* It is directly proportional to the both. Meanwhile, to obtain the minimum threshold current density, a larger wide stripe and smaller characteristic temperature should be selected.

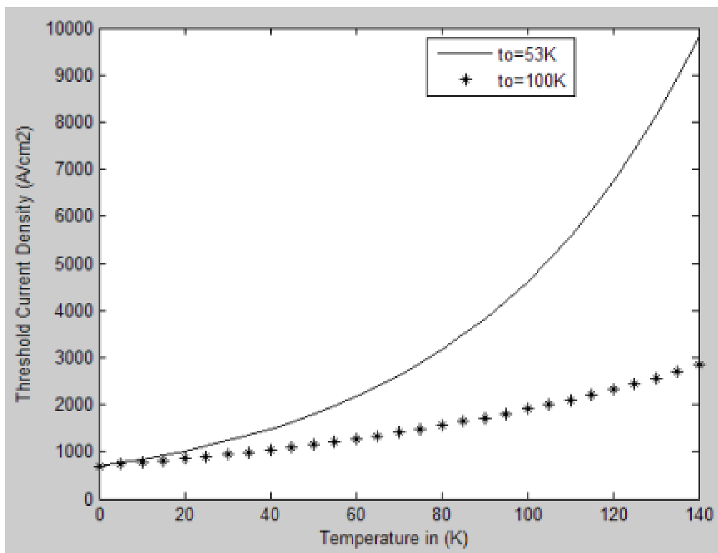

Fig. (6). Threshold current; J_{th} vs T at different T_0 .

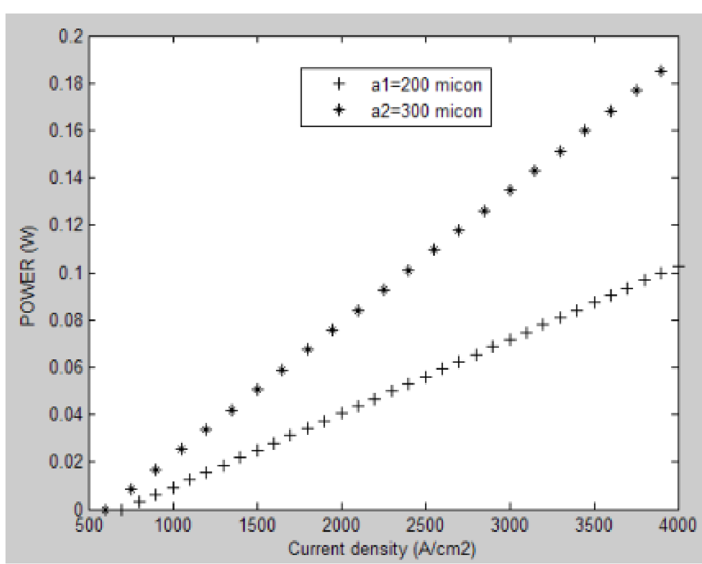

Fig. (7) Radiated Power vs J at different Area.

The high power operation at lower threshold current density is depicted in figures (9, 10 and 11) for pulsed, CW at 14μm and CW at 20μm respectively. By comparison of the previous cases of strip widths, *14, and 20 μm*, one can deduces that as the stripe width is increases; the threshold current reduces. Thereby, the output power was increased and the lasing effects were enhanced.

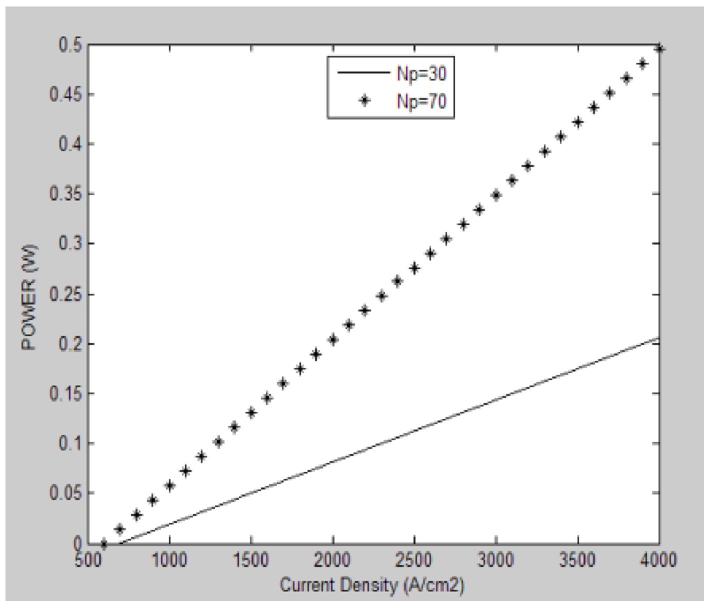

Fig. (8) Radiated Power vs J at different values of Np.

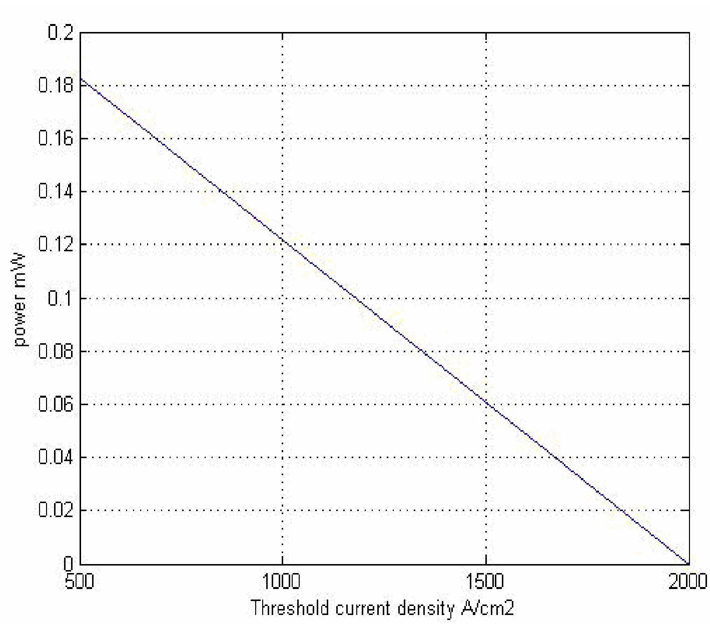

Fig. (9). Radiated Power vs Jth for pulsed operation.

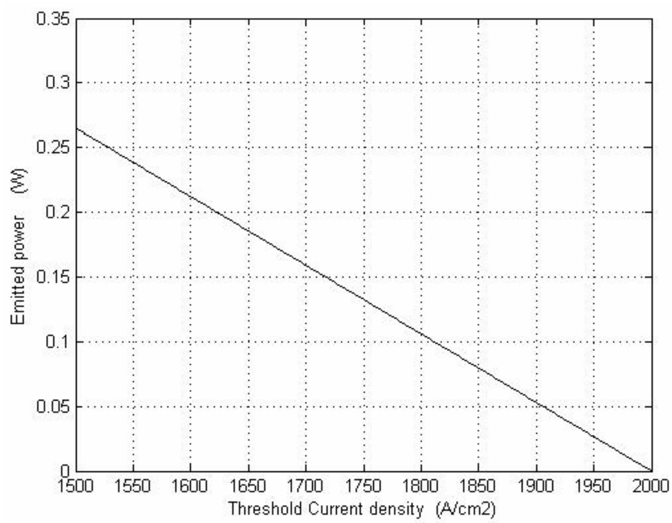

Fig. (10). Radiated Power vs Jth for CW at 14 µm.

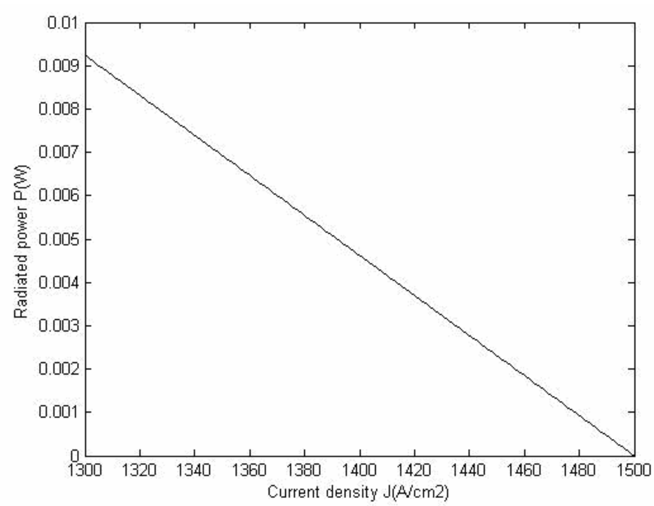

Fig. (11). Radiated Power vs Jth for CW at 20 µm.

The (PW) can be operated over room temperature compared with the (CW) which has a limited operating temperature. This is because of large amount of heat which is dissipated especially with larger stripe widths. In another point of view, when comparing theoretical with practical model, the theoretical emitted optical power behavior is more linear than analogous practical for a wide range of the current density. This may be due to the differences between theoretical and practical internal efficiency and its influence on the waveguide losses.

Finally, equation (2) introduces results that have a good agreement with the practical ones but it is found a little bit discrepancy due to an underestimate of the waveguide losses [18].

5. Conclusion

A mathematical equation that is useful in studying the performance of QCLs is proposed. To ensure the validity of such equation, we make a numerical comparison with the practical results. This comparison is made under the two different cases (PW) and (CW). There is a large matching between the theoretical and practical results. For improving the performance of QCLs; i.e., increasing the amount of radiating power and decreasing the threshold current density, the number of periods N_p and strip area, A, should be increased. The main feature of this study is the influence of the characteristic temperature on the considered figure-of-merits, emitted optical power, and the threshold current density. In turn T_o depends on choosing the compound materials of cascaded structure.

6. References

[1] Mohamed B. El_Mashade, M. Ashry, A. Nasr "Performance analysis of quantum well infrared photodetectors"; *J. of Optical Communications*, Vol.3, pp. 98-110, Germany, Mar. 2005.

[2] Mohamed B. El_Mashade, M. Ashry, A. Nasr, "Theoretical analysis of quantum dot infrared photodetectors"; http://www.iop.org/EJ/abstract/0268-1242/18/9/314, *J. semicond. Sci. Technol*., Vol. 18, pp. 891-900, UK, August 2003.

[3] A. Nasr, Mohamed B. El_Mashade, "Theoretical comparison between quantum-well and dot infrared photodetectors", *IEE Proc. Optoelectronic*, Vol. 153, Issue 4, pp. 183-190, August. 2006.

[4] A. Nasr, A. Aboshosha, S. M. Al-Adl, "Dark current characteristics of quantum wire infrared photodetectors" *IET Proc. Optoelectronic*, Vol. 1, Issue 3, pp. 140-145, April, 2007.

[5] A. Nasr, "Spectral responsivity of the quantum wire infrared photodetectors" *J.Optics & Laser Technology*, Elsevier, Vol. 41, pp. 345–350, 2009.

[6] R. Martini and E.A. Whittaker, "Quantum cascade laser-based free space optical communications", *Journal of Optical and Fiber Communications Reports*, Vol. 2, No. 4, pp. 279-292, 2005.

[7] Federico Capasso , Roperto Paiella,rainer Martini, Raffaele Colombelli,Claire Gmachl,TanyaL.Myers, Matthew s. Taybman,Richard M.Williams,clyde G.Betha, Karl Untrrainer,Harold W.Hwang,Deborah L.Sivco,Alfred W.Cho.,A.Michael Sergent,H.C.Liu,and Edward. A.Whittakei, "Quantum cascade lasers: Ultrahigh-Speed operation, Optical Wireless communication , Narrow Linewidth, and far-infrared Emission", invited paper, *IEEE J. of quantum electronics*, Vol., 38, No.6, pp. 511-532, 2002.

[8] Claire Gmachl, Roberto Paiella, Alessandro Tredicucci, Albert L. Hutchinson, Deborah L. Sivco, James N. Baillargeon,Alfred Y. Cho, and H. C. Liu, "New Frontiers in Quantum Cascade Lasers and Applications", *IEEE J. of Selected Topics In Quantum Electronics*, Vol. 6, No. 6, pp. 931-947, 2000

[9] Giacomo Scalari, "*Magneto-spectroscopy and development of terahertz quantum cascade lasers*", book, Neuchatel, 2005.

[10] Rita Claudia Iotti and Fausto Rossi, "Nature of charge transport in quantum–cascade lasers", *APP. Phys. Lett*., Vol. 78, pp. 2902 -2905, 2001.

[11] Markfox, "*Optical Properties of Solids*", Oxford University press, Ch.6, semiconductor quantum wells, 2001.

[12] Alpes Lasers, "Room Temperature Tunable IR Diode Lasers"**,** *Boston Electronics corporations*, pp. 1-51, 2004.

[13] Govind P. Agrawal, "*Fiber-optic communication systems*", John Wiley & Sons, inc, Ch. 3, optical sources and transmitters, 1992.

[14] Federico Capasso, Alessandro Tredicucci, Claire Gmachl, Deborah L. Sivco, Albert L. Hutchinson, Alfred Y. Cho, and Gaetano Scamarcio, "High-Performance Superlattice Quantum Cascade Lasers", *IEEE J. of Selected Topics In quantum electronics*, Vol. 5, No. 3, pp. 792-807, 1999.

[15] Claire Gmachl, Alessandro Tredicucci, Federico Capasso, Albert L. Hutchinson, Deborah L. Sivco, James N. Baillargeon, and Alfred Y. Cho, "High-power $\lambda \approx 8\mu m$ quantum cascade lasers with near optimum performance", *APP. Phys. Lett*., Vol. 72, No. 24, pp. 3130-3132, 1998.

[16] Mariano Troccoli, David J. Smith, Laurent Diehl and Federico Capasso, "Low-threshold continuous-wave operation of quantum-cascade lasers grown by metalorganic vapor phase epitaxy ", *APP. Phys. Lett*., Vol. 85, No. 24, pp. 5842-5844, 2004

[17] Alessandro Tredicucci, Federico Capasso, Claire Gmachl, Deborah L. Sivco, Albert L. Hutchinson, and Alfred Y. Cho, "High performance interminiband quantum cascade lasers with graded superlattices", *APP. Phys. Lett*., Vol. 73, No. 15, pp. 2101-2103, 1998

[18] Carlo Sirtori , Jerome Fiast , Federeco Capasso ,Deborah L. Sivco,Albert L. Hutchinson, and Alfered Y. Cho, "Quantum Cascaded Laser with Plasma on-enhanced Waveguide Operating at 8.4 µm wavelength", *APP. Phys. Lett*., Vol. 66, No. 24, pp. 3242-3244, 1995.

الخصائص النظرية لمصدر ليزر ذات الكم المتتالي

أشرف سعيد عبد الخالق نصر[١]، محمد بكري المشد[٢]، و محمد الطوخي[٣]

[١]قسم الهندسة الإشعاعية، المركز القومي لبحوث وتكنولوجيا الإشعاع

[١] قسم هندسة الحاسب، كلية الحاسب، جامعة القصيم، هيئة الطاقة الذرية، القاهرة، جمهورية مصر العربية

[٢] قسم الهندسة الكهربية، كلية الهندسة، جامعة الأزهر، القاهرة، جمهورية مصر العربية.

[٣] قسم الهندسة الكهربية – مركز البحوث النووية– هيئة الطاقة الذرية، القاهرة، جمهورية مصر العربية

[١]ashraf.nasr@gmail.com [٣]engtokhy@gmail.com

(قدم للنشر في ٢٠٠٨/١٢/٢٦؛ وقبل للنشر في ٢٠٠٩/٣/١٢م)

ملخص البحث. في هذا البحث, انصب الاهتمام الأساسي على دراسة أداء الليزر ذات الكم المحدد تحت حالتين مختلفتين هما, الموجة النبضية و الموجة المستمرة.وقد وضحت أيضا اعتماد هاتين الموجتين على عناصر هذا النوع من مصادر الليزر. من ثم , تم استنتاج علاقات مقترحة والتي تربط القدرة المنبعثة وأقل تيار مسموح به والكفائة الميلية مع عوامل تركيب هذا النوع من الليزر. ولتحقيق صحة هذه العلاقات, قد تم مقارنة سلوك الخصائص النظرية بالخصائص لعملية. وبالمقارنة , لوحظ أن المعادلات تعطى نتائج شبه متوافقة مع النتائج العملية. وتم بالإضافة إلى ذلك استنتاج تقريب رياضي للقيم الأعلى والأقل للقدرة الضوئية الناتجة.